The International Journal of Advanced Manufacturing Technology (2018) 98:2461–2468
https://doi.org/10.1007/s00170-018-2371-5

ORIGINAL ARTICLE

Tool life and workpiece surface integrity when turning an RR1000 nickel-based superalloy

R. Hood[1] · S. L. Soo[1] · D. K. Aspinwall[1] · A. L. Mantle[2]

Received: 14 March 2018 / Accepted: 22 June 2018 / Published online: 10 July 2018

Abstract
Following a brief review on the turning of nickel-based superalloys, the paper evaluates the machinability and workpiece surface integrity of a powder metallurgy HIP-ed (PHIP) RR1000 alloy, involving two phases of turning experiments using TiN/Al_2O_3/Ti(C,N) coated carbide inserts. Based on a maximum flank wear criteria of 200 μm, tool life exceeded 40 min when operating at or below 100 m/min; however, Taylor tool life curves were extremely steep. At a feed rate of 0.08 mm/rev, workpiece surface roughness was ~0.5 μm Ra. Tests at cutting speeds of 80 m/min or less with new tools showed the 'best/acceptable' surface integrity with no visible white layer or plucking and a maximum distorted layer of ~6 μm deep. In contrast, the surfaces produced using worn tools at a cutting speed of 100 m/min showed a distorted layer of ~20 μm deep with evidence of surface laps and plucking to a depth of ~15 μm.

Keywords Turning · Nickel-based superalloy · Surface integrity

1 Introduction

The ability to maintain much of their strength/integrity and resist corrosion at elevated temperatures (up to ~1000 °C) are key characteristics of nickel-based superalloys and the reason for their extensive use in gas turbine engines for combustion and turbine components [1–3]. As a group however their machinability is poor, the more complex and harder alloys proving more problematic [4, 5] with machining costs typically quoted as ~5 times that for more conventional alloys [4] due in part to low tool life, low productivity and the need to ensure acceptable workpiece integrity. In general, operating parameters when turning include a recommended cutting speed for tungsten carbide tooling of 30–50 m/min [6–8] with an absolute maximum of ~120 m/min [9]. Both single-layer physical vapour deposited (PVD) coatings such as TiAlN and multilayer chemical vapour deposited (CVD) coatings such as TiCN/Al_2O_3/TIN are recommended to allow cutting at higher speeds [10].

Ceramic tooling can also be used including mixed and whisker reinforced alumina, silicon nitride/sialon products and PCBN tools, typically with quoted speeds of ~100–400 m/min [11–13]. When using PCBN to machine Inconel 718 at elevated cutting speeds from 300 to 1500 m/min, Uhlmann and Ederer [14] recommend a reduced cutting speed range of between 400 and 600 m/min in order to avoid excessive tool wear including chipping, the operation also benefiting from specific tool edge chamfer conditions. A comprehensive investigation of machining Inconel 718 with whisker reinforced ceramic tooling at cutting speeds of 100 to 400 m/min showed extensive workpiece surface damage consisting of microcracks, breakage and sideflow with dimensions of up to ~20 μm [15]. Only ~20 of the 72 tests, detailed in this paper, showed a percentage damage area value of less than 15%, which occurred mainly at 100 m/min with new tooling and wet cutting conditions (5 bar and 40 l/min). Other recommendations were that feed rate should range from 0.05 to 0.3 mm/rev depending on the required workpiece surface roughness and that depth of cut should be 0.3 to 0.5 mm when finishing. Despite the potential of ceramics for productivity improvements, increased tooling costs together with adverse workpiece surface integrity and tool reliability issues when finish machining can affect commercial viability.

✉ R. Hood
r.hood@bham.ac.uk

[1] Machining Research Group, Department of Mechanical Engineering, School of Engineering, University of Birmingham, Edgbaston, Birmingham, UK

[2] Manufacturing Technology, Rolls–Royce plc, Derby, UK

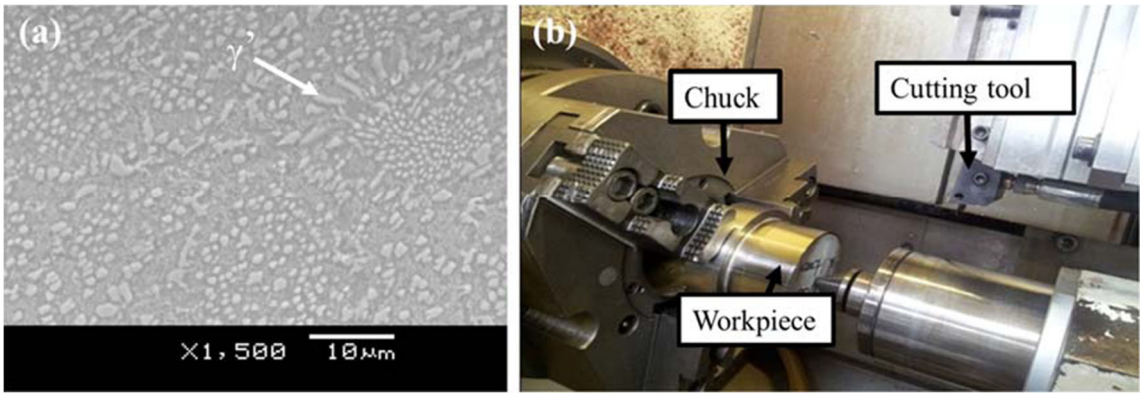

Fig. 1 Experimental details. **a** RR1000 microstructure. **b** Experimental setup

In terms of cutting environment, it is recommended that high pressure fluid with a pressure ranging from 15 to 100 bar with a directed jet should also be used [16]. Dry cutting [17] and MQL use in finish turning [18] have been shown to give poor tool life [17] and high cutting temperatures, with associated workpiece tensile residual stresses [18]. Hybrid laser assisted finish turning of Inconel 718 with ceramic tooling at a cutting speed of 200 m/min, a feed rate of 0.25 mm/rev and depth of cut of 0.25 mm showed a drop in cutting forces along with an improvement in surface finish by over 25% from 0.5 to 0.38 μm Ra compared with more conventional machining practice [19]. Additionally, there was an absence of smeared material together with increased plastic deformation, suggesting compressive residual stresses at the machined surface.

The vast majority of literature found regarding the machinability of nickel-based superalloys refers to forged Inconel 718 in the solution treated and aged condition, reflecting its widespread industrial use and availability. However, the alloy was developed during the 1950s and 1960s [1] and is no longer regarded as leading edge. More recent industrial focus is on alloys produced by powder metallurgy processing, followed by forging or alternatively hot isostatic pressing (HIP), in order to improve mechanical properties or achieve greater economy through near net shape manufacture [20]. A material which is more representative of the current class/generation of nickel-based superalloys is RR1000 which is increasingly being used for turbine discs in gas turbine engines [21]. When produced with a fine grain microstructure, this alloy shows an increase in temperature capability of 25 °C compared with the disc alloy Udimet 720Li [22]. Analysis of the chemical and mechanical properties of RR1000, suggest that it has even lower machinability than current disc alloys including Inconel, Waspaloy or Udimet products [12, 23] and that the operating window for cutting parameters to achieve acceptable tool life, surface roughness and integrity is very narrow. This is due in part to high levels of redeposited material which are found at higher material removal rates or when using cutting inserts with a smaller nose radii. Discontinuous white layers with a thickness of ~ 2 μm which are unacceptable in aerospace applications have also been found when using inappropriate cutting parameters.

Soo et al. [24] investigated both drilling and end milling of PHIP RR1000 with commercially available carbide tooling. Tool performance when drilling with low (30 m/min) or intermediate (45 m/min) cutting speeds was comparable, as both achieved 150 holes without exceeding 100-μm flank wear. Inspection of holes showed hardened layers to a depth of 100 μm along with limited surface anomalies and moderate burring at entry and exit. When milling at a low cutting speed of 25 m/min and feed rate of 0.05 mm/tooth, tool life to reach a maximum flank wear criteria of 200 μm was 120 min; however, white layers were detected in some of the surfaces assessed. The current study aims to complement this work by providing in-depth analysis of the surface integrity of a PHIP RR1000 alloy after turning, which has relevance for the production of components such as casings and discs in gas turbine aero engines.

2 Experimental work

All experiments were conducted on a MHP MT-80 CNC turning centre with a 30-kW motor and a maximum spindle speed of 3000 rpm. The workpiece material was initially supplied in the form of a 'canned' billet (ϕ115 × 315 mm) which had a ~ 4-mm-thick steel skin. Nominal composition was Ni − 15 Cr,

Table 1 Variable parameters for phase 1 tests—tool life and surface roughness

Test number (T)	Cutting speed (m/min)	Feed rate (mm/rev)
T1	80	0.2
T2	120	0.2
T3	100	0.2
T4	80	0.2
T5	100	0.08

Table 2 Variable parameters for phase 2 tests—surface integrity assessment

Surface number (S)	Cutting speed (m/min)	Feed rate (mm/rev)	Tool condition
S1	100	0.2	New
S2	100	0.2	Worn (VB_B max = 200 μm)
S3	100	0.08	New
S4	100	0.08	Worn (VB_B max = 200 μm)
S5	80	0.2	New
S6	80	0.2	Worn (VB_B max = 200 μm)
S7	80	0.08	New
S8	60	0.2	New
S9	60	0.08	New
S10	30	0.2	New
S11	30	0.08	New

18.5 Co, 5 Mo, 3.6 Ti, 3Al, 2Ta, 0.5Hf, 0.03 C, 0.015B and 0.055Zr (percentage by mass) [21]. The material was initially HIP'ed at 1180 °C and 150 MPa for 4 h, then solution heat treated at and subsequently aged to yield a bulk hardness of ~ 450 HV_{30}. An image showing the final microstructure of the workpiece material taken from a section across the bar is given in Fig. 1a. The ends of the billet were electrically discharge wire machined (EDWM'd) and the outer steel casing removed by turning to produce a bar (ϕ110 × 310 mm). The subsequent CNC turning trials were performed on the outside diameter of the bar, see Fig. 1b. Cutting tools were Sandvik Coromant, CNMG 12 04 12-MF S05F (4-μm-thick triple layer TiN/Al_2O_3/Ti(C, N) CVD coated inserts with a fine grain tungsten carbide substrate (~ 1 μm) and ~ 12% Co) [25]. These were held in a Seco Jetstream tool holder: PCLNR2525M12JET, which provided 100 bar water-based fluid emulsion (Houghton Hocut 3380 mineral oil concentration of 7–10%) at 25 l/min during all tests.

Tool wear was measured using a Wild microscope with a toolmakers table with digital micrometre heads giving a resolution of 0.001 mm. Images of tool wear were taken using a digital SLR camera attached to a PC running associated capture software. Workpiece surface roughness was measured using a Taylor Hobson Form Talysurf 120 L with a cut-off length of 0.8 mm and evaluation length of 4.0 mm. For workpiece surface integrity evaluation, selected samples were hot mounted in edge retentive Bakelite, then ground and polished using SiC papers and diamond suspension. A minimum of 500 μm of workpiece material was removed to ensure each sample did not have any damage remaining from the EDWM process used to cut them from the bar. Etching of the samples (for microstructural analysis) was conducted using an electrolytic polishing pen with a solution of 10% ortho-phosphoric acid. Microhardness measurements (depth profile) were taken using a Mitutoyo 810 hardness testing machine using a Knoop indenter at 50 g load and indent time of 15 s. Three measurement profiles on each section were taken, at 10 μm intervals from the surface until bulk hardness was achieved. The average for each depth was calculated and plotted. Selected machined workpiece surfaces and cross-sections were analysed using a Leica optical microscope running Buehler Optimet software, together with a JEOL 6060 scanning electron microscope to assess the level of workpiece damage.

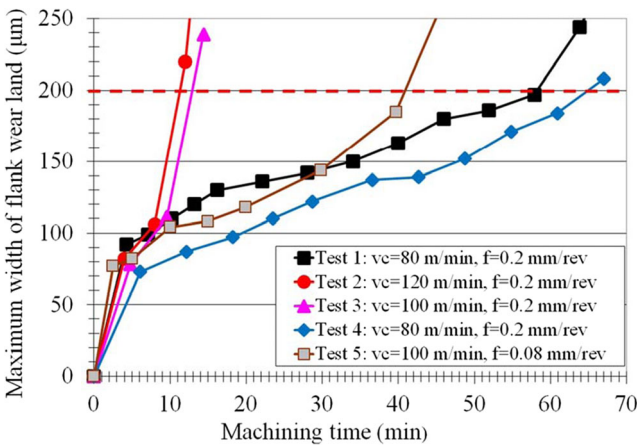

Fig. 2 Maximum width of flank wear land against machining time

Two phases of experimental work were undertaken, the first (phase 1) involving evaluation of tool life and workpiece roughness (Ra measurements taken parallel to the feed direction with the average calculated), using a matrix of operating parameters based on tool supplier information and literature review data. See Table 1 for test details. T1, T2 and T3 investigated the effect of cutting speed within the range 80 to 120 m/min. T4 was a replication of T1 and used to assess the repeatability of T1. Only a single replication was possible due to limited material supply and this was selected as the preferred operating condition. T5 used a lower feed rate of 0.08 mm/rev with a cutting speed of 100 m/min. Phase 2 research detailed in Table 2 assessed workpiece surface integrity via microscopy analysis of surface topography, sub surface microstructure and microhardness depth profiles. Phase 2 work mainly focused on surfaces hence they are denoted by S rather than T. Surfaces from both new and worn tools are denoted by S1, S2 etc. Samples S1 to S6 (and their associated surfaces) were produced using phase 1 test parameters; however, samples 7 to 11 were generated using lower operating parameters. Under such conditions, tool life would be expected to be long (~ 100 min plus) and therefore due to insufficient time and workpiece material, life trials were not performed; consequently, only surfaces produced with new tools were evaluated. In both phases of work, the depth of cut was held constant at 0.25 mm to represent finishing conditions, as any component would be produced near net shape thus eliminating the requirement for extensive roughing operations. The criterion for end of tool life was a maximum flank wear of 200 μm in view of the safety critical nature of the likely

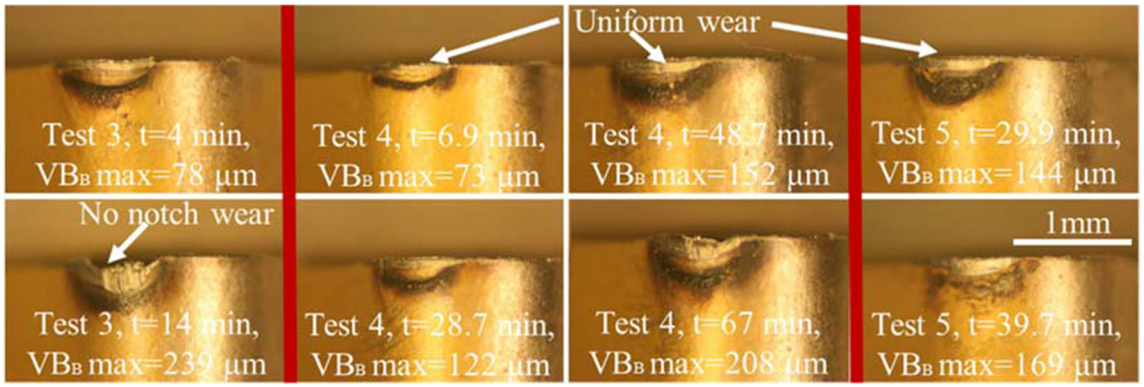

Fig. 3 Tool wear scar photographs

component application and the requirement for desirable surface integrity [2].

3 Results and discussion

3.1 Tool life and wear

Phase 1 tool life results showing the maximum width of flank wear land against machining time are given in Fig. 2. The traces show typical wear profiles with a period of rapid initial wear until ~80 µm followed by more gradual flank wear progression. Tests T3 and T2 at 100 and 120 m/min respectively provided short lives of less than 13 min; however, a tool life in excess of 60 min was possible using a cutting speed of 80 m/min and a feed rate of 0.2 mm/rev. Tool life was reasonably consistent between the T1 and T4 replication, with a difference of 15%. Natural variability was potentially one reason for the different, the material was supplied with a 'steel skin' and potentially, there were differences between the outside and centre of the bar. In order to preserve workpiece material, a detailed analysis of the material properties of the bar was not completed. It is not possible to make detailed conclusions concerning the performance of the alloy under replication as workpiece material supply is extremely scarce.

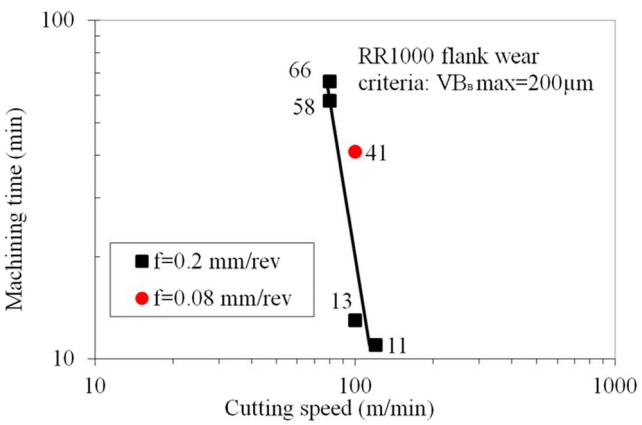

Fig. 4 Velocity-time (vT) curve

A reduction in feed rate from 0.2 to 0.08 mm/rev produced an increase in tool life from 13 to 41 min. Li et al. [26] reported that higher tensile residual stresses of up to 900 MPa were produced using worn tooling rather than new when face turning RR1000 washers produced from disc forgings. They concluded that excessive tool wear must be avoided to reduce these high levels of tensile stress which would be detrimental to fatigue performance. The good tool life performance in the current study is therefore encouraging for the production of components with acceptable integrity.

Selected wear scar photographs for tests T3, T4 and T5 are shown in Fig. 3. Wear format was similar for all tests with the majority of wear being uniform; no significant notch wear was seen. Additional in-depth analysis of wear mechanisms was beyond the scope of the current study; however, when turning Inconel 718 at cutting speeds between 50 and 100 m/min and feed rates of 0.075 to 0.125 mm/rev at a depth of cut of 0.25 mm, Bhatt et al. [10] found abrasive and adhesive wear mechanisms to be the most dominant. The authors also suggest that tool life was short with only 8 min of operation at a cutting speed of 100 m/min, although it would appear that the trials were performed dry.

Velocity-time curves (vT) are useful at illustrating and comparing the effect of operating parameters on tool life;

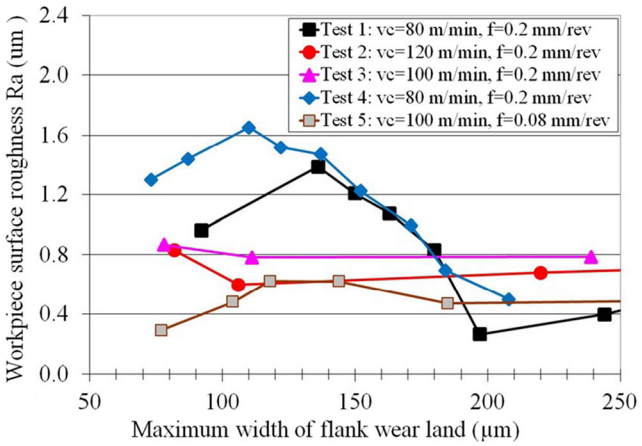

Fig. 5 Surface roughness Ra against maximum flank wear for phase 1

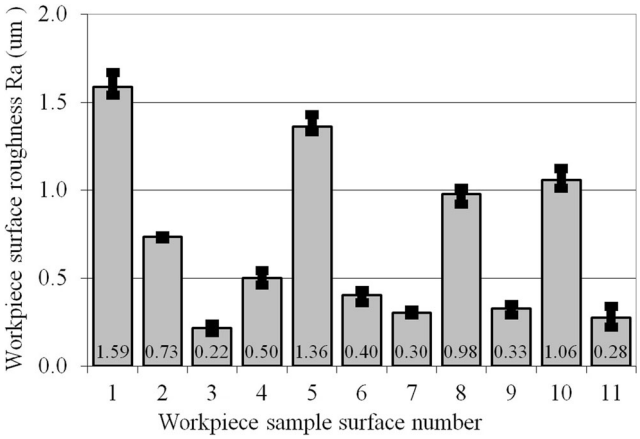

Fig. 6 Workpiece surface roughness Ra for each workpiece surface sample in phase 2

however, their use in publications discussing the machinability of nickel-based superalloys is limited. Figure 4 shows a vT curve for the cutting speed range 80–120 m/min in the current study based on the flank wear criteria of 200 μm. It is

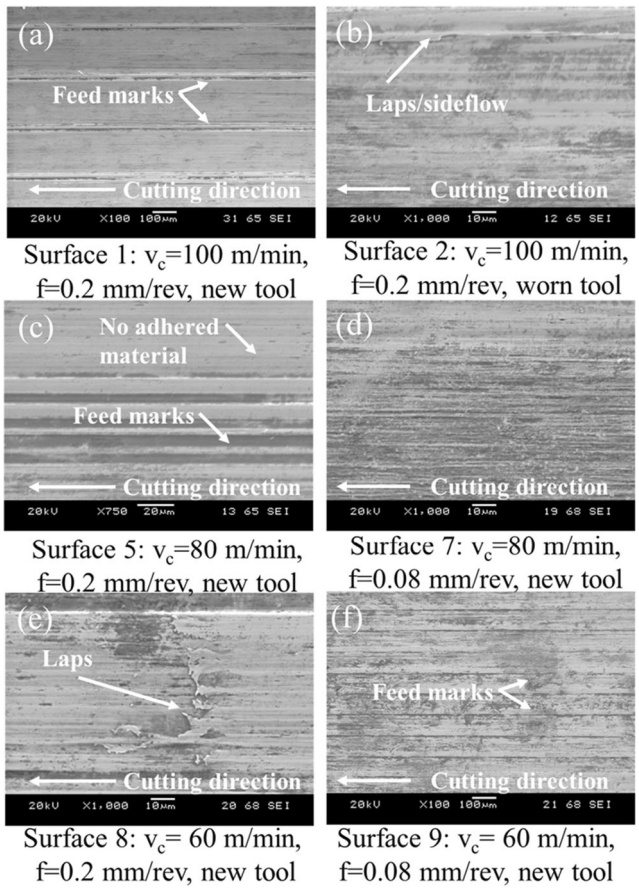

Fig. 7 Images of the turned workpiece sample surfaces. **a** Surface 1: v_c = 100 m/min, f = 0.2 mm/rev, new tool. **b** Surface 2: v_c = 100 m/min, f = 0.2 mm/rev, worn tool. **c** Surface 5: v_c = 80 m/min, f = 0.2 mm/rev, new tool. **d** Surface 7: v_c = 80 m/min, f = 0.08 mm/rev, new tool. **e** Surface 8: v_c = 60m/min, f = 0.2 mm/rev, new tool. **f** Surface 9: v_c = 60 m/min, f = 0.08 mm/rev, new tool.

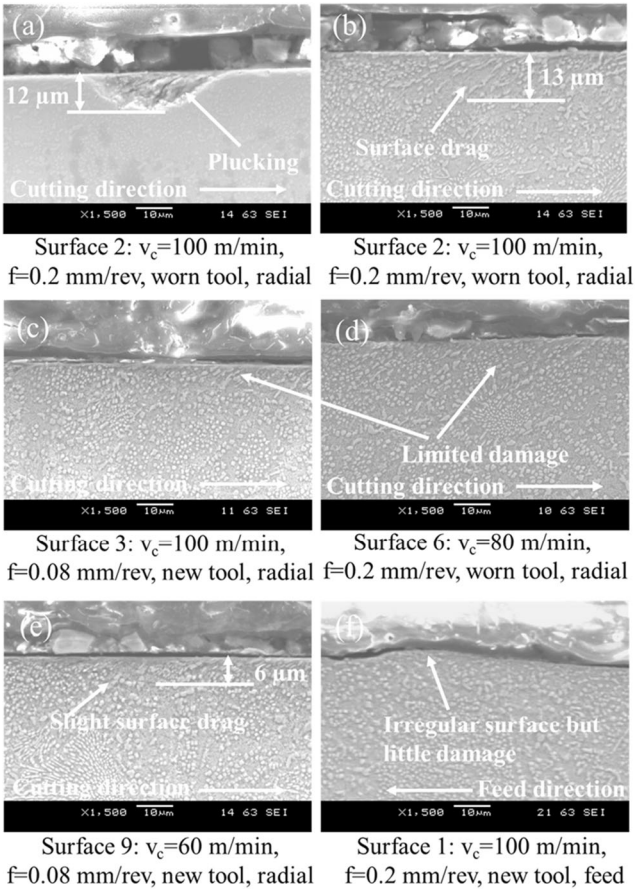

Fig. 8 Secondary electron images of the workpiece sample surface/subsurface. Samples were electrolytically etched with a solution of 10% ortho-phosphoric acid. **a** Surface 2: v_c = 100 m/min, f = 0.2 mm/rev, worn tool, radial. **b** Surface 2: v_c = 100 m/min, f = 0.2 mm/rev, worn tool, radial. **c** Surface 3: v_c = 100 m/min, f = 0.08 mm/rev, new tool, radial. **d** Surface 6: v_c = 80 m/min, f = 0.2 mm/rev, worn tool, radial. **e** Surface 9: v_c = 60 m/min, f = 0.08 mm/rev, new tool, radial. **f** Surface 1: v_c = 100 m/min, f = 0.2 mm/rev, new tool, feed

extremely steep ($vT^{0.23} = 200$), indicating that the choice of cutting speed is critical to maximising tool life. A similar trend was reported by Axinte et al. [12] with an extremely narrow operating parameter region when machining RR_X obtained by the powder metallurgy route. A cutting speed of 100 m/min reducing the feed rate from 0.2 to 0.08 mm/rev increased the time to reach the tool life criteria from 13 to 41 min.

3.2 Workpiece surface roughness

A wide range of surface roughness (Ra) values were obtained using phase 1 operating parameters, with a maximum roughness ~ 1.6 μm Ra and a minimum of ~ 0.3 μm Ra, lower values being associated not unrealistically with the use of the low feed rate of 0.08 mm/rev, see Fig. 5. Tests T1 and T4 showed a similar response with an increase in roughness within the first 150 μm of flank wear followed by a reduction to < 0.5 μm Ra. In contrast, tests T2, T3 and T5 showed only a

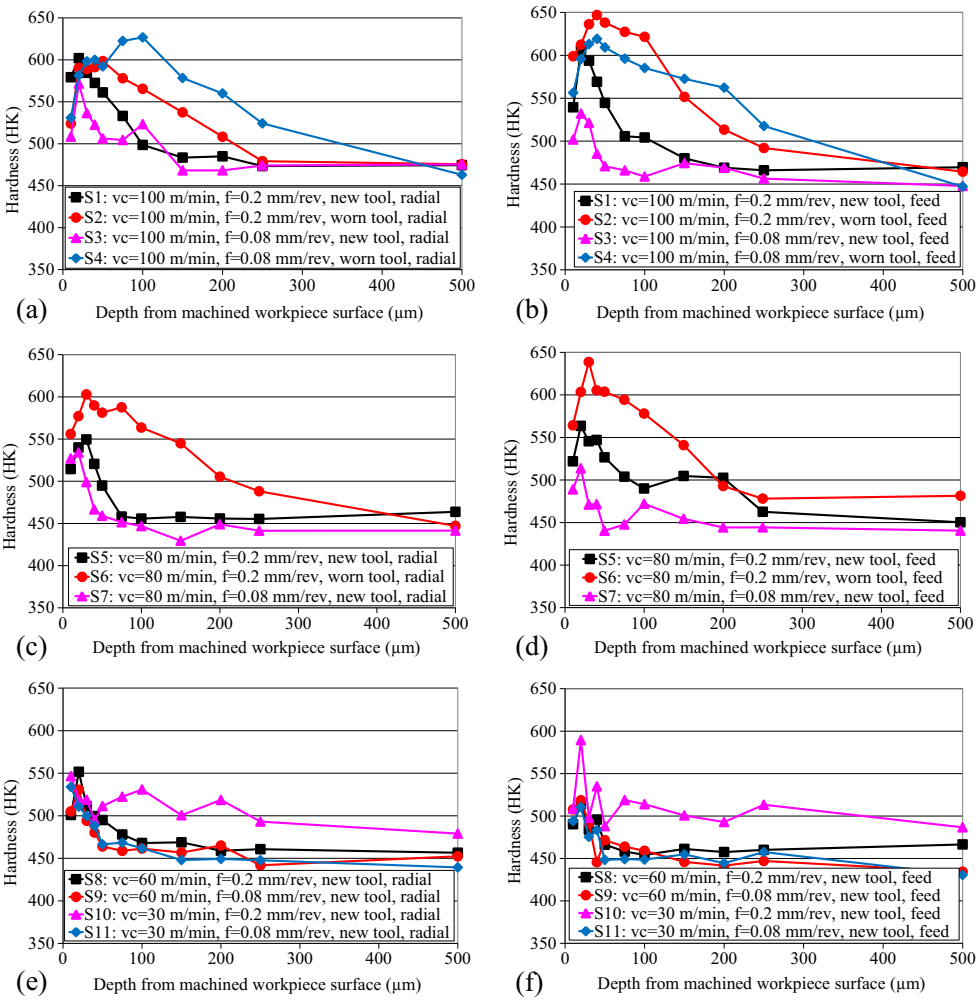

Fig. 9 Hardness against depth from the machined surface. **a**, **c** and **e** Radial direction. **b**, **d** and **f** Feed direction

limited difference in roughness as flank wear increased. Figure 6 shows the results of phase 2 tests with a similar wide range in surface roughness values from 0.22 to 1.59 μm Ra as a consequence of the various operating levels and edge wear conditions. In general, new tools produced a higher roughness than worn tools, which was possibly due to nose/edge radius wear [27]. At a cutting speed of 100 m/min, Ra reduced from 1.59 to 0.22 μm, with feeds of 0.2 and 0.08 mm/rev when using new tools. In general, a decrease in cutting speed from 100 to 30 m/min using a feed rate of 0.2 mm/rev (samples 1, 5, 8 and 10) reduced surface roughness by ~33%.

3.3 Workpiece surface integrity

Images of turned surfaces from phase 2 taken using the JEOL 6060 SEM are shown in Fig. 7. Typically, when using new tools, feed marks, which were either 0.2 or 0.08 mm apart (depending on the feed rate used), were visible on every surface, see Fig. 7a, c and f for S1, S5 and S9, but less noticeable on surfaces produced using the lower feed rate. Similar feed marks were reported by Zhu et al. [15]. In addition, redeposited material/laps were evident, see Fig. 7b, e which were visible along the feed marks and were generally smaller than 10 μm wide but up to 100 μm long.

Subsurface cross-sections provided in Fig. 8 showed no visible white layer formation either in the feed direction or radial direction, suggesting that conditions even at higher cutting speeds were relatively conservative. This is in contrast to the work of Axinte et al. [12] who reported a ~3-μm white layer. The present lack of microstructural change in the region very close to the surface was possibly due to improved fluid application; however, operating parameter differences may also have had an effect and masked the results. Processing differences between the two alloys will also have had an effect as well. Unfortunately, the parameters given by Axinte et al. [12] were coded and therefore difficult to establish; however, the use of 6 bar fluid application contrasts sharply with the 70 bar directed flow arrangement in the present work. Literature review comments highlighted cutting fluid as a critical concern when machining nickel-based superalloys, the use of higher pressures allowing effective penetration of the cutting fluid into the interface between the tool flank and the

machined surface leading to lower levels of rubbing and cutting temperature, resulting in lower tool wear and improved surface roughness [3]. It is also likely that high pressure fluid reduced the level of workpiece material adhesion to the turned surface as indicated by the lower levels observed on the surface, shown in Fig. 7 and the cross-sectional micrographs in Fig. 8.

Several instances of plucking (~25 μm wide and ~15 μm deep) were found on surfaces in the radial direction for S2 (v = 100 m/min, f = 0.2 mm/rev, worn tool) and one instance for S4 (v = 100 m/min, f = 0.8 mm/rev, worn tool). Figure 8a shows an example of this type of damage. The redeposited material shown in Fig. 7 was not evident to any great extent in the sample sections analysed; however, several instances of a distorted layer/surface drag were found in the radial direction. Higher operating parameters (cutting speed, feed rate) and flank wear level caused increased grain distortion levels up to ~20 μm deep, see Fig. 8b. At lower operating parameters (surfaces S8 to S11), such deformation was < 6 μm deep, see example in Fig. 8e, while surfaces appeared smoother in the radial direction than in the feed direction. Surfaces S1 and S3 produced with new tools and high feed rate had cyclic peaks and troughs 0.2 mm apart, while surfaces produced with worn tools showed a smoother profile than those made using new tools.

Figure 9 shows microhardness (HK) depth profiles for all samples (S1 to S11) in phase 2 tests, machined in both the radial and feed directions. Hardened layers with a depth of up to 400 μm and magnitude of up to 650 HK were measured depending on the operating parameters used. In general, a higher cutting speed, feed rate and flank wear level resulted in a hardened layer with greater magnitude and depth, with tool wear appearing as the critical factor. In all surfaces used to compare new and worn tooling (samples 1 and 2 (v = 100 m/min, f = 0.2 mm/rev), samples 3 and 4 (v = 100 m/min, f = 0.08 mm/rev) and samples 5 and 6 (v = 80 m/min, f = 0.2 mm/rev)), the worn tool produced a hardened layer which extended deeper into the workpiece surface and had a higher magnitude of up to 50 HK than a new tool. Cutting speed had a lower effect on the hardened layer. Using identical operating parameters, only the samples produced with a cutting speed of 100 m/min showed any increase in hardness level and depth when compared to the other speeds (80, 60 and 30 m/min). Knowledge of the depth of the hardened layer is important for post-processing operations such as shot peening, which are often used to remove unwanted tensile residual stresses [28].

4 Conclusions

- The machinability of the PHIP nickel-based superalloy RR1000 has been established when turning with coated carbide tools. Recommendations for production of surfaces with desirable integrity have been established.
- When operating at v_c = 80 m/min, f = 0.2 mm/rev and v_c = 100 m/min, f = 0.08 mm/rev, a tool life in excess of 30 min (flank wear criteria of 200 μm) was achieved. The vT curve for cutting speeds of 80 to 120 m/min at a feed rate of 0.2 mm/rev was extremely steep, indicating that the choice of cutting speed is critical in maximising tool life.
- Testing at the lower feed rate of 0.08 mm/rev with a cutting speed of 100 m/min produced a surface roughness of 0.3 to 0.5 μm Ra over the life of the insert.
- In phase 2, operating with new tools at 30, 60 and 80 m/min produced the 'best' surface integrity with no visible white layer or plucking. Additionally, the distorted layer did not exceed ~6 μm in depth. Surfaces produced using worn tools at a cutting speed of 100 m/min did however show plucking and grain distortion up to ~15 and 20 μm deep respectively.

Acknowledgements The authors would like to thank Rolls–Royce plc and in particular to Dr. Wayne Voice for the provision of workpiece material and technical advice. Additional thanks are due to Sandvik Coromant for the supply of tooling and Seco Tools for supply of the Jetstream tool holders.

References

1. Reed RC (2006) The Superalloys fundamentals and applications. Cambridge University Press, Cambridge
2. M'Saoubi R, Axinte D, Soo SL, Nobel C, Attia H, Kappmeyer G, Engin S, Sim WM (2015) High performance cutting of advanced aerospace alloys and composite materials. CIRP Ann Manuf Technol 64(2):557–580
3. Thakur A, Gangopadhyay A (2016) State-of-the art in surface integrity in machining of nickel-based super alloys. Int J Mach Tool Manu 100:25–54
4. Richards N, Currie AM, Aspinwall DK, Smith DJM, Dewes RC (1996) Tool life data when machining nickel based alloys with ceramic cutting tools. In: Proceedings of the thirteenth conference of the Irish manufacturing committee, IMC-13, University of Limerick, Ireland, 4–6 September 1996:13–21
5. Ulutan D, Ozel T (2011) Machining induced surface integrity in titanium and nickel alloys: a review. Int J Mach Tools Manuf 51:250–280
6. Ezugwu EO (2005) Key improvements in the machining of difficult-to-cut aerospace alloys. Int J Mach Tools Manuf 45:1353–1367

7. Xue C, Chen W (2011) Adhering layer formation and its effect on the wear of coated carbide tools during turning of a nickel-based alloy. Wear 270:895–902
8. Sharman ARC, Hughes JI, Ridgway K (2015) The effect of tool nose radius on surface integrity and residual stress when turning Inconel 718™. J Mater Process Technol 216:123–132
9. Yazid MZA, Che-Haron CH, Ghani JA, Ibrahim GA, Said AYM (2011) Surface integrity of Inconel 718 when finish turning with PVD coated tools and MQL. Procedia CIRP 19:396–401
10. Bhatt A, Attia H, Vargas R, Thomson V (2010) Wear mechanisms of WC coated and uncoated tools in finish turning of Inconel 718. Tribol Int 43:1113–1121
11. Nalbant M, Altin A, Gokkaya H (2006) The effect of cutting speed and cutting tool geometry on machinability properties of nickel-base Inconel 718 super alloys. Mater Des 28(4):1334–1338
12. Axinte DA, Andrews P, Li W, Gindy N, Withers PJ (2006) Turning of advanced Ni based alloys obtained via powder metallurgy route. CIRP Ann Manuf Technol 55(1):117–120
13. Zhou JM, Bushlya V, Peng RL, Johansson S, Avdovic P, Stahl J-E (2011) Effects of tool wear on subsurface deformation of nickel-based superalloy. Procedia CIRP 19:407–413
14. Uhlmann E, Ederer G (2001) High speed turning of Inconel 718. Ind Diam Rev 61(/3):169
15. Zhou JM, Bushlya V, Stahl J-E (2012) An investigation of surface damage in the high speed turning of Inconel 718 with use of whisker reinforced ceramic tools. J Mater Process Technol 212:372–384
16. Ezugwu EO, Bonney J, Fadare DA, Sales WF (2005) Machining of nickel-base, Inconel 718, alloy with ceramic tools under finishing conditions with various coolant supply pressures. J Mater Process Technol 162–163:609–614
17. Outerio JC, Pina JC, M'Saoubi R, Pusavec F, Jawahir IS (2008) Analysis of residual stresses induced by dry turning of difficult-to-machine materials. CIRP Ann Manuf Technol 57:77–80
18. Kamata Y, Obikawa T (2007) High speed MQL finish-turning of Inconel 718 with different coated tools. J Mater Process Technol 192-193:281–286
19. Attia H, Tavakoli S, Vargas R, Thomson V (2010) Laser assisted high-speed finish turning of superalloy Inconel 718 under dry conditions. CIRP Ann Manuf Technol 59:83–88
20. Silva JM, Claudio RA, Brito SE, Branco CM, Byrne J (2006) Characterization of powder metallurgy (PM) nickel base superalloys for aeronautical applications. Mater Sci Forum 514–516:495–499
21. Hessel SJ, Voice W, James AW, Blackham SA, Small CJ, Winstone MR (1997) Nickel alloy for turbine engine component, European Patent Specification, EP 0 803 585 B1. European Patent Office, Int Cl. C22C 19/05. Application number: 97302518.2. Date of filing: 14/04/1997. Date of publication: 09/02/2000.
22. Hardy MC, Zirbel B, Shen G, Shankar R (2004) Developing damage tolerance and creep resistance in a high strength nickel alloy for disc applications. In: Proceedings of the 10th International Symposium on Superalloys (Superalloys 2004), Pennsylvania, USA 83–90
23. Seco Tools, Material Background—The essential material characteristics of RR1000, www.secotools.com/de, accessed 2015
24. Soo SL, Hood R, Aspinwall DK, Voice WE, Sage C (2011) Machinability and surface integrity of RR1000 nickel based superalloy. CIRP Ann Manuf Technol 60(1):89–92
25. Sandvik Coromant, Sandvik Coromant grades information sheet, 2016
26. Li W, Withers PJ, Axinte D, Preuss M, Andrews P (2009) Residual stresses in face finish turning of high strength nickel-based superalloy. J Mater Process Technol 209:4896–4902
27. Khidhir BA, Mohamed B (2010) Machining of nickel based alloys using different cemented carbide tools. JESTEC 5/3:264–271
28. International Organization for Standardization (1993) ISO 3685 Second edition 1993-11-1 Tool-life testing with single point turning tool